Peertechz

Annals of Mathematics and Physics

Annals of
Mathematics and Physics
OPEN ACCESS JOURNAL

ISSN: 2689-7636 Journal DOI: https://dx.doi.org/10.17352/amp

Mini Review

Research and Development of New Vibration and Noise Reduction Methods and their Manufacturing Technology

Levan Gavasheli[1]* and Anri Gavasheli[2]

[1]Professor, Academy of Physical and Mathematical Sciences, Tbilisi, Georgia

[2]Bachelor of Science in Economics with Mathematical Concentration, Drexel University, Philadelphia, USA

Submitted : 19 February, 2026
Accepted : 25 February, 2026
Published : 26 February, 2026

***Corresponding author:** Levan Gavasheli, Professor, Academy of Physical and Mathematical Sciences, Tbilisi, Georgia, E-mail: levan_gavasheli@yahoo.com

Keywords: Vibration isolation; Flexible-damping materials; Nonlinear mechanical systems; Hysteresis behavior; Drilling machinery

https://www.mathematicsgroup.us

Abstract

Based on the theoretical research conducted in our laboratory, a technology for producing new flexible-damping materials has been developed. These flexible-damping elements are characterized by an increased ability to absorb harmful energies and high resistance to cyclic loads, while under static and dynamic loads, their 'stress-displacement' behavior exhibits a hysteresis characteristic in a hyperbolic form. These advantages of flexible-damping elements allow them to be effectively used in the production of vibration- damping devices for heavy machinery, where vibration levels often exceed permissible limits, especially when operating in harsh environmental conditions.

Introduction

Presented by us is the design of one type of top-down shock absorber, which is shown in Figure 1. The top-down shock absorber is used for the effective vibration protection of heavy drilling machines and their mechanisms [1]. The top-down shock absorber consists of the following parts: detachable upper (1) and lower (2) parts of the housing, drive shaft (3), upper (4) and lower (5) parts of the flexible damping element, support tube (6), yoke (7), upper (8) and lower (9) connectors, and the expanded end part of the shaft (10). During the operation of the shock absorber, the acting external stress is calculated using the formula

$$P = P_0 + q\cdot\ell + m(\ell) + \left(\frac{\ell P_1}{n\pi}\right)^2,$$

Where P_0 – there is axial load, $q \cdot l$ – its own weight, (ml) and $l \cdot P_1$ components of the centrifugal force, n– is the number of cyclic loads.

Parts: 3 – drive cam; 4 and 5 – upper and lower elements of the flexible damping element; 6 support tube; 7-lever; 8 and 9 – upper and lower couplings; 10 – expanded end of the cam.

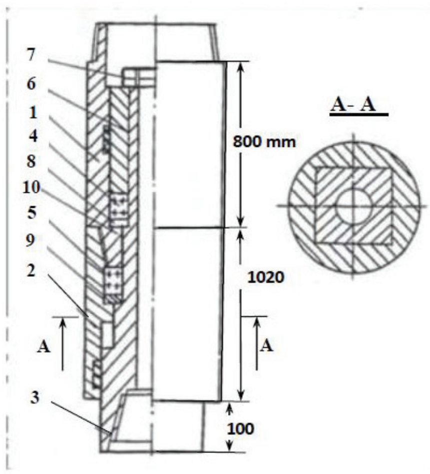

Figure 1: Explodable top 1 and bottom 2 of the shock absorber housing.

The critical value of angular velocity generated during loading is calculated using the formula,

$$v_{kr} = \left(\frac{n\pi}{\ell}\right)^2 \cdot \sqrt{\frac{m(\ell)}{E\ell}},$$

Where E is the modulus of elasticity of the vibration-damping material in dynamic mode. Based on theoretical research, a new technology for the production of elastic-damping materials has been developed. The mentioned elastic-damping elements used in this system are characterized by an increased ability to absorb harmful energies and high resistance to cyclic loads. For the transmission of torque, a square section is used on the shaft and the lower part of the housing, as shown in the first drawing with section A-A [2].

The operating principle of the vibration isolator is as follows: the axial load from the drill rig's drill pipe is transferred to the upper part of the housing 1, then through the upper flexible damping elements 4, as well as through the spindle 3 - to the lower flexible-damping elements 5 and through the lower part of the housing 2 to the main working part - the drilling tool. The upper 4 and lower 5 flexible-damping elements are pre-compressed with a certain force, which in turn prevents vibration shocks of the drilling tool and the entire system to the drilled rocks. Within the framework of the experiment, we determined the shape of the static cyclic loading unloading hysteresis loop of the flexible-damping elements, which is shown in Figure 2.

Simultaneously, we developed methodologies for determining the use of flexible-damping elements under operational conditions, their characteristics, and main working parameters, which make it possible to evaluate the service life and efficiency of flexible-damping elements under mandatory vibration conditions. The advantages of these flexible-damping elements allow them to be used in heavy machinery, specifically heavy drilling equipment with complicating factors, where the vibration levels significantly exceed permissible sanitary and hygienic standards, especially when operating in challenging environmental conditions, for the production of effective vibration protection solutions. Drilling equipment to determine and record the levels of mechanical forced vibrations and harmful vibrations of the drilling equipment, we used a field vibrometer and a vibration recorder (Danish company Brüel & Kjær). Piezoelectric accelerometers of the DH-3M1 type were mounted at the site of origin of the harmful vibrations, and their operating scheme is shown in Figure 3.

The operating principle of the piezoelectric accelerometer is as follows: a force $P = ma$, generated as a result of mechanical

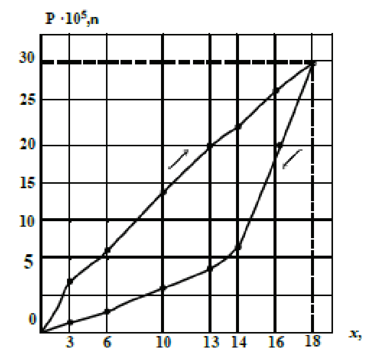

Figure 2: Hysteresis loop form of static cyclic load-unload of flexible-damping elements.

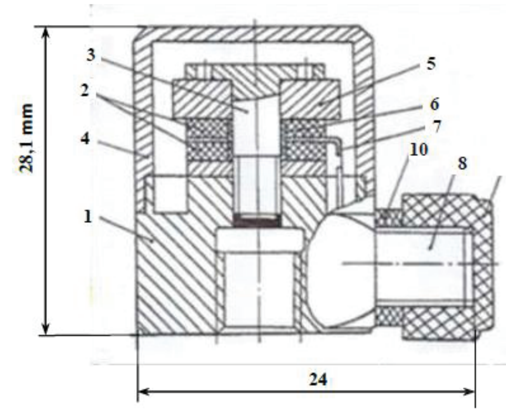

Figure 3: Structural diagram of the piezoelectric accelerometer manufactured by the Danish company "Bruel & Kjaer": 1 - base; 2 - piezoelectric element; 3 - shaft; 4 - cover; 5 - inertial mass; 6 and 7 - electrical potential contact wires; 8 - wires for electrical power supply; 9-protective cap;10-protective ring [3].

vibrations based on the piezoelectric effect, where a is the vibration acceleration and m is the inertial mass, causes deformation of the piezoelectric element, which results in electrical charges on the surface of the piezoelectric element. These charges are proportional to the force acting at a fixed moment and to the correspondingly generated vibration acceleration.

The operating frequency range of the piezoelectric accelerometer is calculated using the formula

$$f_n = \frac{0,79}{R(C_n + C_0)}$$

where C_n - is the volumetric capacity of the vibro-generator, in farads; and C_o - is the voltage capacity within it, in farads,

$$R = \frac{R_n \cdot R_0}{R_n + R_0},$$

where R_n - the electrical resistance of the vibrator, omi; R_o - the electrical resistance of the amplifier included in it, omi; n- cyclic deformation number [4].

Based on the analysis of experimental results, we determined that in the tested devices, the vibration level during the operation of the vibration damping means decreased on average by 12 – 14 dB in each vibration band, and the resonant frequency of the vibration damping means ranged between 120 – 125 Hz. The logarithmic levels of the vibration velocities are shown in Figures 4,5 [5].

The logarithmic levels of vibration velocities at the operator's workplace of the equipment in octave bands without x_1, y_1, z_1, and with the use of vibration damping devices x_2, y_2, z_2 are presented in the Table 1.

Processing of experimental data obtained from numerous measurements when working with the vibration protection device shows that the dynamic loads on the working component of the mechanical system and on the operator's workplace are reduced and stabilized. In addition, the mechanical operation

Citation: Gavasheli L, Gavasheli A. Research and Development of New Vibration and Noise Reduction Methods and their Manufacturing Technology. Ann Math Phys. 2026;9(1):040-043. Available from: https://dx.doi.org/10.17352/amp.000178

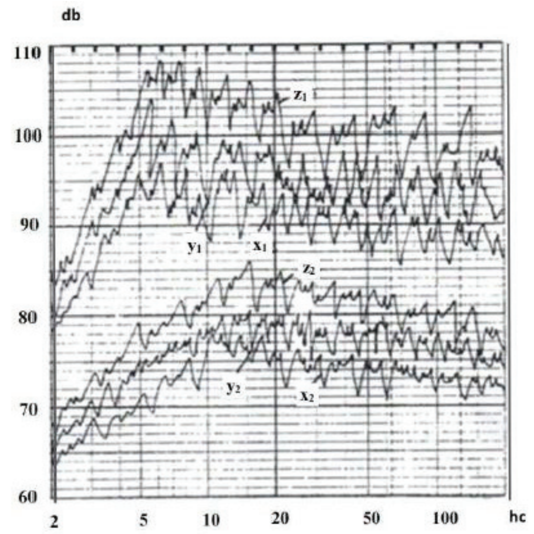

Figure 4: Logarithmic levels of vibration velocities at the drilling machine operator's workplace in the directions of the x_1, y_1, z_1 axes without the operation of the machine's vibration damping device; and in the directions of the x_2, y_2, z_2 axes with the vibration damping device in operation.

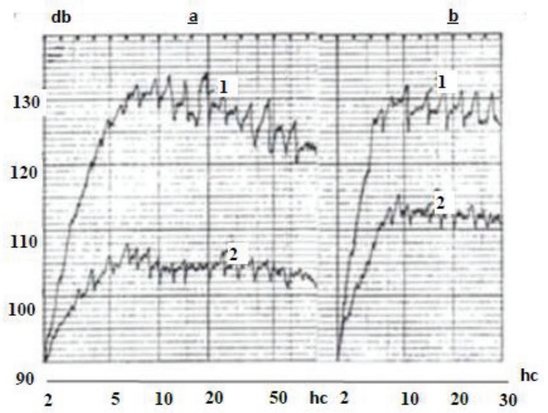

Figure 5: Logarithmic levels of vibration velocities on the drilling rig spindles and directly on the drill *a* – 1, *b* - 1, without the vibration damping device of the rig; *a* – 2, *b* - 2, with the vibration damping device of the rig.

Table 1: Vibration velocity levels, dB

Process Name	Direction	Mean geometric frequency band, Hz					
		2	4	8	16	31,5	63
Without a vibration dampening device	x_1	104	107	101	99	96	90
	y_1	102	104	103	96	95	93
	z_1	105	109	104	98	97	92
In case of using an antivibration device	x_2	96	93	90	83	80	81
	y_2	100	92	91	88	86	83
	z_2	97	95	93	85	84	85
		108	99	93	92	92	92

speed increases by 35% and the service life of the working component increases by 30%. These results are achieved due to the smooth and automatic adjustment of the stiffness of the elastic-damping element in the vibration protection device.

The mechanical model of the body of a seated machine operator with a vibration protection device is shown in the figure 6.

Using the mechanical model of the seated operator, it was possible to determine its amplitude-frequency characteristic: a - in the vertical direction; b - in the horizontal direction, Figure 7.

The efficiency of the vibration damping device K_{ef} - is determined as follows

$$K_{ef.} = \frac{\alpha_0}{\alpha_1},$$

where α_0-- vibration acceleration without the use of a vibration damping device; α_1-- vibration acceleration when using a vibration damping device. In addition, when ω > 1,41, ω_0

where ω - is the frequency of forced vibrations, ω_0- is the natural frequency of vibrations, then the use of a vibration damping device is effective and the levels of vibration acceleration

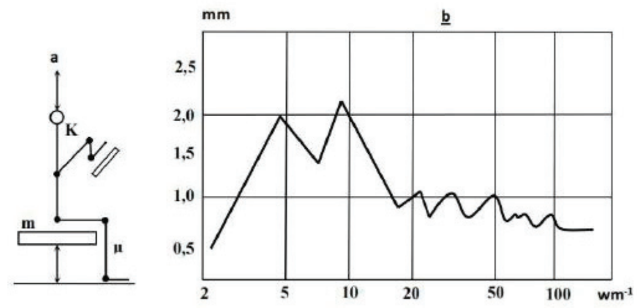

Figure 6: a - mechanical model of a seated operator; b- amplitude-frequency characteristic of a seated operator $m = \frac{5}{7}(80-100)$, kg - combined mass of the operator and the vibration damping device; *K*- Average stiffness of the operator's chest and arms, $K \approx 5{,}63 \cdot 10^3\,\mathbf{N/m}$; ì coefficient of blunt friction of the operator's body, $\mu \approx 52{,}5,\ \mathbf{N \cdot s/m}$.

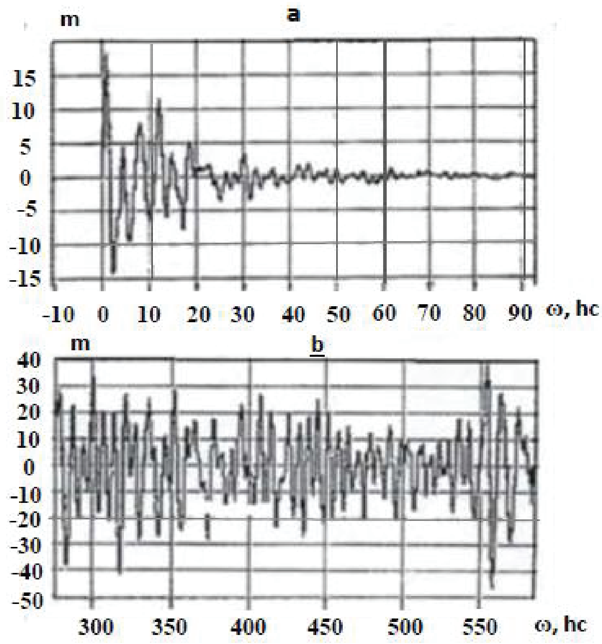

Figure 7: Amplitude-frequency characteristic of a seated machinist: *a* - in the vertical direction; *b* - in the horizontal direction.

Citation: Gavasheli L, Gavasheli A. Research and Development of New Vibration and Noise Reduction Methods and their Manufacturing Technology. Ann Math Phys. 2026;9(1):040-043. Available from: https://dx.doi.org/10.17352/amp.000178

(vibration velocity) are significantly reduced when using the vibration damping device, when

$$\frac{\omega}{\omega_0} < 1{,}41\,,$$

The system operates completely inefficiently, and the occurrence of self-excitation and, consequently, resonance modes is not excluded. The logarithmic levels of vibration velocities in the average geometric frequency bands at the drill rig operator's workplace in the directions of the x_1, y_1, z_1 axes without using the rig's vibration damping device; and in the directions of the ; x_2, y_2, z_2 axes when using the rig's vibration damping device, are given in Table 2.

Table 2: Vibration velocity levels, dB.

Process Name	Direction	Mean geometric frequency band, Hz					
		2	4	8	16	31,5	63
Without a vibration dampening device	x_1	102	106	100	98	94	88
	y_1	100	102	105	97	95	92
	z_1	104	110	103	96	96	90
In case of using an antivibration device	x_2	98	94	90	84	82	82
	y_2	100	95	92	90	85	84
	z_2	99	93	92	86	83	80
		108	99	93	92	92	92

Conclusion

Obviously, in our case

$$\frac{\omega}{\omega_0} > 1{,}41\,,$$

This means that the use of a vibration damping device is effective. This fact K_{ef} > 1 once again confirms the validity of the main parameter values of the flexible-damping elements determined as a result of the theoretical studies we conducted.

References

1. Gavasheli LS. Theory of vibration protection of nonlinear mechanical systems. Tbilisi: Metznireba; 2006;272.
2. Gavasheli LS, Makharadze LI. Transverse damping of main pipelines of hydrotransport systems under the influence of parametric forces. Georgian Eng News. 2016;(2):59-62.
3. Metrikine AV, Hagedorn P. Influence of bending-torsion coupling on the vibration of elastic structures. J Sound Vib. 2002;252(4):619-638.
4. Rao SS. Mechanical vibrations. 6th ed. Harlow: Pearson Education; 2017. Available from: https://www.amazon.in/Mechanical-Vibrations-Singiresu-S-Rao/dp/013436130X
5. Nayfeh AH, Mook DT. Nonlinear oscillations. Weinheim: Wiley-VCH; 2008. Available from: https://www.wiley.com/en-us/Nonlinear+Oscillations-p-9783527617593

Citation: Gavasheli L, Gavasheli A. Research and Development of New Vibration and Noise Reduction Methods and their Manufacturing Technology. Ann Math Phys. 2026;9(1):040-043. Available from: https://dx.doi.org/10.17352/amp.000178